CHEMISTRY

Invoking Polymer Order: High Magnetic Field Orientation of Liquid Crystalline Thermosets

Benicewicz, B.C., Center for Polymer Synthesis, Rensselaer Polytechnic Institute
Smith, M.E., LANL
Earls, J.D., Dow Chemical Co.
Priester, R.D., Jr., Dow Chemical Co.
Douglas, E.P., UF, Materials Science and Engineering
Duran, R.S., UF, Chemistry
Setz, S.M., UF, Chemistry

Our current work at the NHMFL is focused on using high magnetic fields to create highly oriented polymers, and then controlling the processing parameters to translate the high orientation into high mechanical properties. Liquid crystalline thermosets have been studied as a route to achieving this goal. Maximum enhancement in properties of liquid crystalline thermosets depends on the ability to create orientation in a preferred loading direction. The orientation process is dependent on the liquid crystalline nature of the fluid phase since it is the cooperative effects of the molecules that gives rise to magnetic field orientation of organic molecules at these field strengths. The material used in experiments at the NHMFL is 4,4'-diglycidyloxy-alpha-

methylstilbene cured with sulfanilamide. The initially isotropic material forms a smectic liquid crystalline phase during the crosslinking process.

Experiments were conducted to define the effects of high magnetic fields on the orientation and mechanical properties of LCT's cured in the field. In particular, the effects of polymerization temperature and catalyst type on the orientation and mechanical properties of the final cured polymer were examined. Mechanical property measurements were made both parallel and transverse to the magnetic field direction. In the first set of experiments, temperature effects between 150 °C and 180 °C were investigated. A significant decrease in mechanical properties was found at the higher temperatures. Although we could not conclude that there were differences between the samples cured at 150 °C and 160 °C, the moduli measured at 180 °C in a 2.0 T field were quite low. It was concluded that the higher temperatures were too close to the isotropization temperature of the smectic fluid, and the loss in orientation dominates the process at this temperature. In the second set of experiments, a faster catalyst was used and compared to the previous work on a slower catalyst. For the conditions examined in this study, no significant differences were found between the two catalysts. The orientation process appears to occur at a rate faster than the polymerization. Until recently, only limited data has been measured and reported for the tensile moduli in the direction transverse to the magnetic field direction. We conducted a more complete evaluation of this effect. The transverse tensile moduli were found to be representative of the normal property level for high performance materials of this type, and is contrary to the result for liquid crystalline polymers where orientation in a preferred direction leads to a significant decrease in the transverse direction. The ability to maintain conventional mechanical properties in the transverse direction while increasing properties in a preferred direction appears to be an unusual and potentially beneficial property of liquid crystalline thermosets.

We have defined the effects of several key processing variables for achieving orientation, and enhanced mechanical properties in liquid crystalline thermoset polymers. These results will be incorporated into our experimental testing protocol for further testing at field strengths in the critical range of 1 T to 3 T.

Laser-Polarized Xenon-129 NAMR and BET Isotherm Analysis of Xe Absorption on Lyophilized Proteins

Bharatam, J., UF, Chemistry
Storhaug, V., UF, Chemistry
Webster, C.E., UF, Chemistry
Cottone, A., III, UF, Chemistry
Gianna, R., UF, Chemistry
Bowers, C.R., NHMFL/UF, Chemistry
Gaffney, B.J., NHMFL/FSU, Biology

Technology for preparing hyperpolarized xenon-129 by spin-exchange optical pumping has led to recent polarization transfer techniques in NMR, including thermal mixing, Hartmann-Hahn matching, and nulcear Overhauser effect (NOE) effect. We report studies of Xe binding to lyophilized proteins using hyperpolarized Xe-129 NMR. Three low mw proteins, for which Xe binding information is available from NMR[1], and/or x-ray studies (metmyoglobin, methemoglobin, and lysozyme), and one large protein with an internal cavity, not previously studied for Xe binding (lipoxygenase), were examined. Lipoxygenase exhibited an adsorbed Xe NMR peak at 5 ppm at 233 K, and at 55 ppm at 148 K, as shown in Figure 1. The other proteins exhibited much smaller shifts of the surface-associated signal. Additionally, BET isotherms were obtained. The 77 K nitrogen isotherms demonstrated surface areas of 23.3 m^2/g, 12.9 m^2/g, and 504 m^2/g for myoglobin, lysozyme, and lipoxygenase, respectively. The Xe isotherms at 210 K also showed substantially greater binding by lipoxygenase. We hypothesize that the large internal channel in lipoxygenase contributes to the differences in surface area by permitting gas molecules greater access to the internal surface of the protein. To test

this, we anticipate future experiments wherein signals from nuclei on the surfaces of proteins, or in hydrophobic cavities, might be enhanced by polarization transfer from Xe.

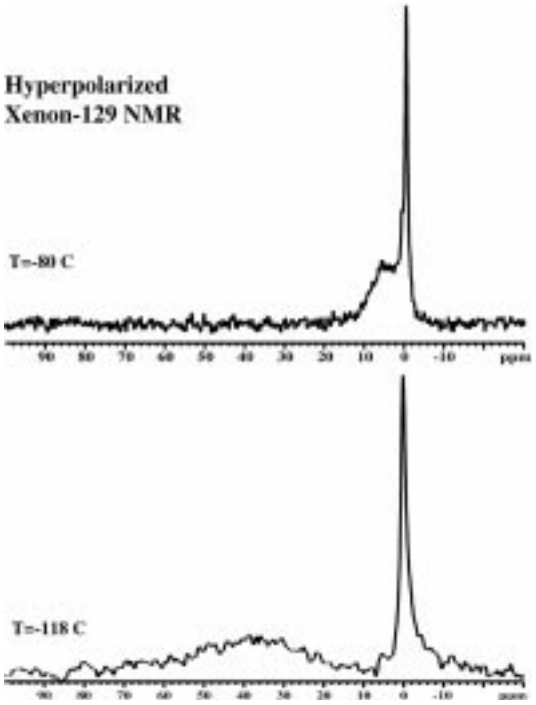

Figure 1. Hyperpolarized xenon-129 NMR spectra of xenon adsorbed onto lyophylized lipoxygenase protein at two different temperatures. The broad component shifted from 5 ppm to 40 ppm upon changing the temperature from -80 to -118 C. This peak represents xenon associated with the surface of the protein.

Reference:

1 Tilton, R.F., *et al*., Biochem., 21, 6850-6857 (1982).

Phase Transitions, Molecular Packing, and Dynamical Modes in Reentrant Nematic Liquid Crystals: A Xenon-129 NMR Investigation

Bharatam, J., UF, Chemistry
Bowers, C.R., NHMFL/UF, Chemistry

The ability to detect and characterize nematic reentrance by xenon-129 NMR chemical shift and spin relaxation data is demonstrated in several different reentrant nematic liquid crystal mixtures. In Figure 1 we present the xenon-129 spin-spin relaxation time temperature dependence for xenon dissolved a certain two-component liquid crystal mixture. The activation energies of the dominating spin relaxation process in the nematic and reentrant nematic phases are derived from the temperature dependence of the spin relaxation times. The results for the binary and tertiary reentrant nematic liquid crystal mixtures are compared in terms of the molecular packing and dynamical modes responsible for nuclear spin relaxation.

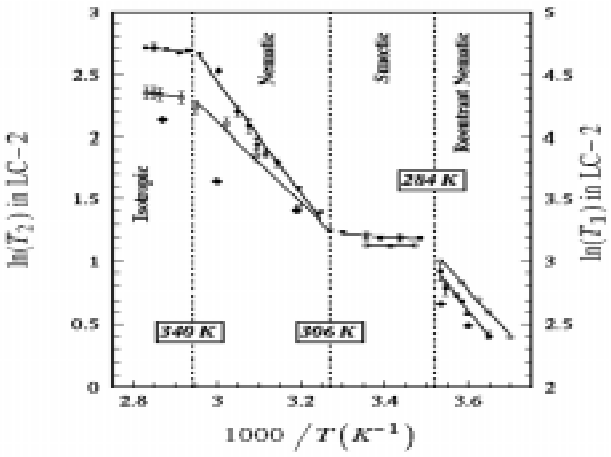

Figure 1. The reciprocal temperature dependence of the spin-lattice (square symbols, axis at right) and spin-spin (circles, axis at left) relaxation times for xenon-129 dissolved in a reentrant nematic liquid crystal, recorded at 11.7 T. The diamonds indicate spin-lattice relaxation values recorded at a field of 9.40 T. The temperatures at which phase transitions are known to occur in this system are indicated by dashed vertical lines. The absence of error bars on some data points indicates that the error in the measurement is less than the size of the symbol. Solid lines indicate linear regression fits to the data in each phase. The slopes yield the activation energy of the motion dominating the relaxation.

A High Field EPR Study of Canthaxanthin Radical Cations Stabilized on Silica-Alumina Surfaces

Bratt, P.J., NHMFL/UF, Chemistry
Konovalova, T.A., Univ. of Alabama, Chemistry
Kispert, L.D., Univ. of Alabama, Chemistry
Brunel, L.-C., NHMFL
Krzystek, J., NHMFL

Carotenoids play an important role as initiators in the photochemistry of photosynthetic processes. They have the dual functions of accessory pigments in energy capture and transferring to the reaction centers, and of deactivating reactive forms of oxygen. These compounds are often involved in electron transfer reactions in photosynthetic reaction centers resulting in carotenoid radical cation formation ($Car^{\bullet+}$). These radical cations, which are generated electrochemically, are unstable in solution, but are stable when stabilized on silica-alumina surfaces even at room temperature as a result of the formation of electron transfer complexes between adsorbed carotenoid molecules and Al(III) Lewis acid sites on the surface. The electron transfer reactions of carotenoids adsorbed on a surface, where the carotenoid motion is restricted, is expected to be a good model for such reactions in the photosynthetic reaction center where carotenoids are surrounded by proteins.

Although the X-Band EPR spectrum is a single unresolved line, the 326 GHz EPR spectrum exhibits a degree of asymmetry. Spectral simulation indicated that this was due to *g*-anisotropy, where $g_{||} = 2.0034$ and $g_{\perp} = 2.0023$, and is shown in Figure 1. This type of *g*-tensor is consistent with current theory for polyacene π-radical cations, which states that the *g*-tensor becomes cylindrically symmetrical with increasing chain length. Appearance of cylindrical symmetry is consistent with the Stone theory for polyacenes. From the comparison of the *g*-tensor obtained in these experiments with those observed for cation radicals in doped crystals, this indicates that the carotenoid radical does not occur in a stacked array with the electron exchange existing along this stack. This also demonstrates that the symmetrically unresolved EPR line at X-Band is due to a carotenoid π-radical cation with the electron density distributed throughout the entire chain as predicted by RHF-INDO/SP molecular orbital calculations.[1,2] The lack of temperature dependent EPR line widths are suggestive of rapid rotation of methyl protons even at 5 K, which average out the proton couplings from three oriented ß-protons. Simulations of EPR spectra at 95 GHz, 140 GHz, and 250 GHz, give only symmetrical unresolved lines. This allows the estimation of the lower limit of the frequency of rotation for methyl groups, which is predicted to be greater than 350 GHz.

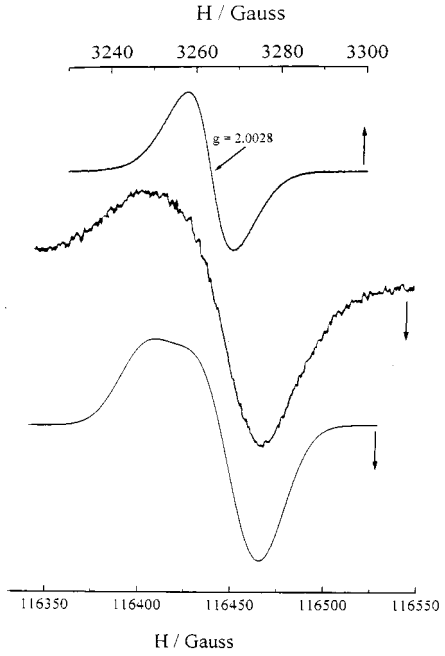

Figure 1. (a) X-band EPR spectrum of canthaxanthin radical cation adsorbed on the surface of activated silica-alumina at 77 K; (b) high field EPR spectrum of the same sample at 326 GHz and 5 K; (c) simulated 326 GHz spectrum.

This work was supported by the Division of Chemical Sciences, Office of Basic Energy Sciences, Office of Energy Research, the U.S. Department of Energy, Grant DEFG05-86ER13465.

References:

1 Plato, M., *et al.*, Chem. Phys., 107, 185 (1986).
2 Lendzian, F., *et al.*, Chem. Phys. Lett., 148, 377 (1988).

Conformations of Peptide Fragments from the FK506 Binding Protein: Comparison to the Native and Urea-Unfolded States

Callihan, D.E., NHMFL/FSU, Chemistry
Logan, T.M., NHMFL/FSU, Chemistry

The helix-forming tendency of seven peptide fragments corresponding to the entire sequence of the FK506 binding protein (FKBP) has been investigated in aqueous buffer, and in 2,2,2-trifluoroethanol (TFE) using CD and NMR spectroscopy. All fragments exhibited random coil conformations in aqueous buffer, but the amount of helix induced in the peptide fragments by TFE varied. The fragment with the highest intrinsic helicity corresponded to the single α-helix in native FKBP. Fragments corresponding to β-strands 2 and 3 also exhibited strong propensity towards helix formation. In contrast, the fragment corresponding to β-strand 1 did not form a helix in TFE.

The inherent helix-forming tendencies are interpreted in light of the native structure to suggest possible folding nucleation sites. Conformational sampling in each peptide fragment was also compared to that observed in unfolded FKBP. With the exception of the fragment corresponding to β-strand 2, the formation of helical structures in the peptide fragments in TFE was correlated with the observation of turn and/or helix conformers in urea-unfolded FKBP. Surprisingly, peptide fragments in aqueous solution were less structured than the corresponding regions in the unfolded FKBP. The conformational differences between the peptide fragments and unfolded FKBP were not due to the urea buffer, or to differences in their rotational correlation times, but did require a solvent environment of lowered polarity.

How, then, might a long polypeptide chain promote the formation of transient secondary structure when shorter peptide fragments can not? Hydrodynamically, denatured proteins are spherical, with hydrodynamic radii (R_h) larger than native proteins and molten globule intermediates, but smaller than that expected for an ideal random coil.[1] The hydrophobic interactions in the unfolded protein are not strong enough to generate a compaction, as in a molten globule or compact folding intermediate, but may result in a polarity differential such that, on average, the inside of the expanded sphere is less polar than the outside.[2,3]

We propose that formation of non-random secondary structures in an unfolded protein to promote chain segments that have an inherent tendency towards helix formation, through transient contacts with non-polar chain segments that lower the polarity of the local environment. These interactions are likely to be important in the earliest stages of protein folding.

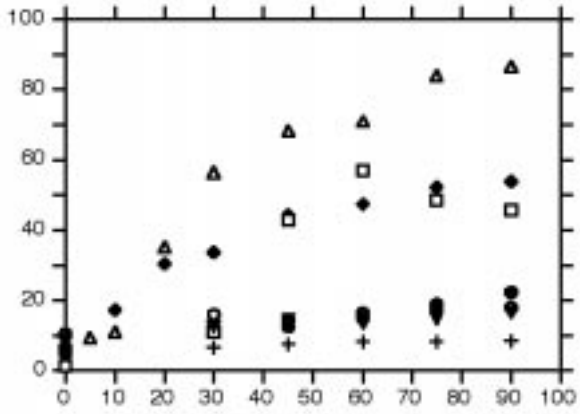

Figure 1. Change in average percent helix in seven peptide fragments from FKBP with TFE.

References:

1 Pan, H., *et al*., Protein Sci., 6, 1985-1992 (1997).
2 Chalikian, T.V., *et al*., J. Mol. Bio., 250, 291-306 (1995).
3 Makhatadzhe, G.I., J. Mol. Bio., (1992).

Modulating Dipoles for Structure–Function Correlations in the Gramicidin A Channel

Cotten, M., NHMFL/FSU, Chemistry
Tian, C., NHMFL/FSU, Molecular Biophysics
Busath, D.D., Brigham Young Univ., Zoology
Cross, T.A., NHMFL/FSU, Chemistry and Molecular Biophysics

Long-range electrostatic interactions are much more important in membrane proteins than in water soluble proteins, because of the low dielectric constant of the bilayer interstices. The indole side chains of tryptophan bear a substantial dipole, and this may be an important reason for why tryptophans are much more common in membrane proteins than in water soluble proteins. Here, we have studied the influence of these dipoles in the polypeptide, gramicidin A, which as a dimer forms a monovalent cation selective channel across lipid bilayers.

It has previously been shown, that the sum of the monopole–dipole interactions between the indole dipoles (four of them), and the cation at the channel and bilayer center accounts for a factor of 20 in ion conductance rate. These interactions occur over an interaction distance of 1.0 nm to 1.3 nm, and yet, they are clearly important for the channel function. Only with the knowledge of a high resolution structure has it been possible to accurately define the interaction magnitudes. For gramicidin the indole ring orientations are known to within a couple of degrees with respect to the channel axis.

Now, we have modified the indole dipole moments by fluorinating the indole ring at different positions. By deuterating the remaining carbon sites in the indole, and observing the ^2H spectra of these sites (see Figure 1), it has been possible to confirm that fluorination has had only a small effect (less than 10°) on the orientation of the individual indoles with respect to the channel axis, despite large changes in dipole magnitude and orientation. As predicted, the changes in the dipole moments have lead to changes in the conductance properties of the channel as determined by single channel conductance measurements. Indeed, it has been possible to enhance the efficiency for ion conductance through these subtle modifications to the channel.

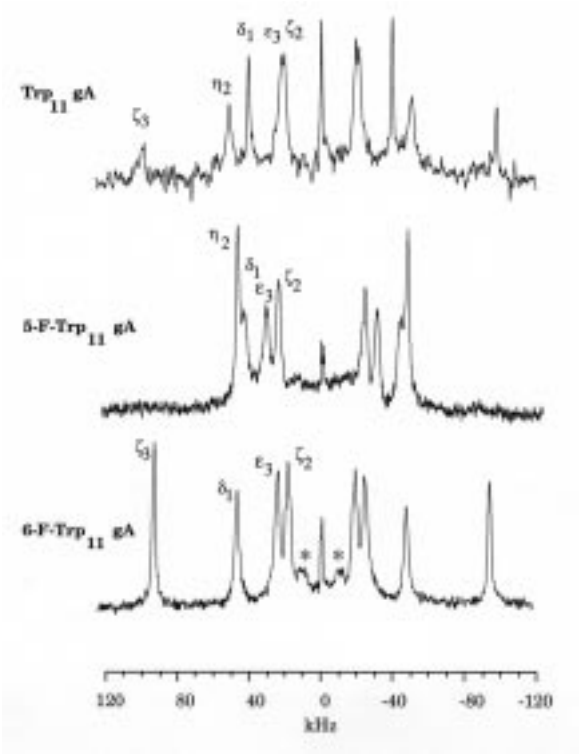

Figure 1. ^2H spectra obtained at 92 MHz of ring-d5-Trp_{11} (top spectrum), ring-d4-5F-Trp_{11} (middle spectrum), and ring-d4-6F-Trp_{11} (bottom spectrum) labeled gramicidin in uniformly aligned lipid bilayers. All expected quadrupolar splittings are observed, and the relatively narrow linewidths are consistent with an orientational spread of as little as 1° in the time-averaged orientation of the indole ring with respect to the magnetic field direction.

Such long range electrostatic interactions do not play a major role in the protein function of water soluble proteins, because the higher dielectric constant of the environment screens the influence of the dipoles. In membrane proteins, the transport of ions and polar molecules across the membrane is an essential and common activity. The role of these electrostatic interactions will be a common theme, requiring high resolution structural information to elucidate. To date, solid state NMR is the only technique that has been demonstrated to have sufficient resolution for such an analysis.

Multifrequency EPR of Ultramarine Blue

Eaton, S.S., Univ. of Denver, Chemistry and Biochemistry, and Engineering
Eaton, G.R., Univ. of Denver, Chemistry and Biochemistry, and Engineering
Quine, R.W., Univ. of Denver, Chemistry and Biochemistry, and Engineering
Rinard, G.A., Univ. of Denver, Chemistry and Biochemistry, and Engineering
Krzystek, J., NHMFL
Hassan, A., NHMFL
Brunel, L.C., NHMFL

Ultramarine blue (a brilliant deep-blue solid) has been used as a reference material for EPR, since its g value is well-separated from g = 2, the line width is ca. 17.5 G at X-band at room temperature, and it does not saturate readily.[1] X-ray and neutron diffraction, together with MAS NMR, confirmed the previously proposed sodalite structure for ultramarine blue, but with Si and Al in the framework disordered.[2] The consensus of prior EPR studies is that the EPR signal in ultramarine blue is due to the S_3^- radical, and that in "pure" ultramarine blue the signal is exchange-narrowed yielding a line that is Lorentzian in the central region of the spectrum.[3] The goal of the present study is to test the model that the S_3^- radical in ultramarine blue is undergoing rapid motion by examining the spectrum of the radical in ultramarine blue by CW EPR over a wider range of microwave frequencies and sample temperatures than have been used previously.

An international team of scholars, with access to several EPR frequencies, is collaborating on this study, which is in its preliminary stages. EPR spectra from 258 MHz to 35 GHz were run in Denver, and spectra from 108 GHz to 670 GHz were run at the NHMFL. W-band and higher frequency EPR spectra were stimulated by the observation of wider EPR lines at Q-band than at X-band. Since prior work indicated that the spectra were exchange-narrowed in the central part of the line, and that the g-value dispersion was of the order of 0.05, it was thought that the anisotropy observed as a line distortion at Q-band might be resolved at a field strong enough to overcome the exchange narrowing. It is especially striking that the line shape is nearly Lorentzian at frequencies between 0.259 GHz and 35 GHz, even though the line width differs by about a factor of 2 in this frequency range at room temperature.

EPR spectra of the S_3^- radical center in ultramarine blue over a factor of about 2500 in frequency (258 MHz to 670 GHz), and as a function of temperature at some frequencies do not exhibit resolution of g anisotropy. The line width decreases from 258 MHz to 2.7 GHz, then stays approximately constant to ca. 9 GHz, above which the width increases with frequency. It is suggested that even at liquid helium temperature there is rapid motion of the S_3^- radical in the cages of the aluminosilicate lattice resulting in averaging of anisotropies and spin exchange with neighboring S_3^- radicals, and that these rates are fast relative to the EPR Zeeman frequency.

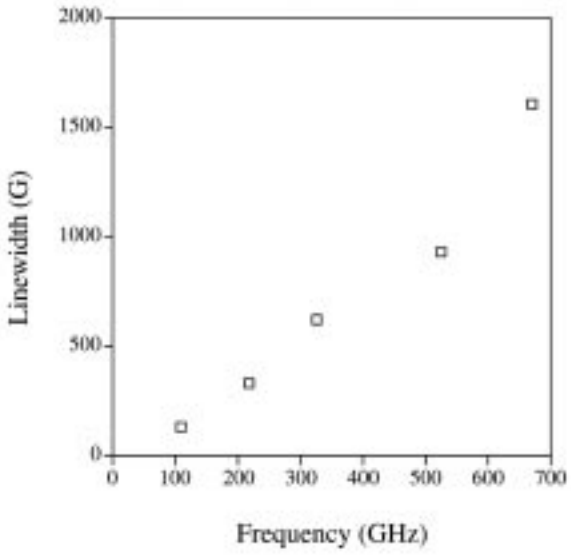

Figure 1. EPR linewidth of ultramarine blue as a function of frequency in the high frequency regime (above 100 GHz).

This work was supported by NSF grant DIR9316827 (GRE), NIH grant GM21156 (GRE), NIH grant GM57577 (GAR), and by the NHMFL.

References:

1 Brown, D.W., *et al.*, J. Phys. Chem., 66, 2602 (1962).
2 Tarling, S.E., *et al.*, Acta Cryst. B, 44, 128 (1988).
3 Gobeltz, N., *et al.*, J. Chem. Soc. Faraday, 94, 677 (1998).

Analysis of Combinatorial Libraries Using Electrospray Fourier Transform Ion Cyclotron Resonance Mass Spectrometry

NHMFL

Eyler, J.R., NHMFL/UF, Chemistry
Watson, C.H., UF, Chemistry
Benner, S.A., UF, Chemistry
Wigger, M., Swiss Federal Institute of Technology, Chemistry
Li, W., FSU, Chemistry
Marshall, A.G., NHMFL/FSU, Chemistry

Electrospray ionization (ESI) coupled with Fourier transform ion cyclotron resonance (FTICR) mass spectrometry has been used to explore certain biological/chemical aspects of combinatorial libraries. The work was carried out both at UF and at the NHMFL, primarily by graduate student Maria Wigger. Significant results have been obtained when examining various peptide/receptor interactions and in actual screening experiments where a receptor binds (interactions are mainly due to non-covalent interaction) to a few library components (those with the highest binding constants). A combination of mass spectrometry and IRMPD fragmentation has been found to have sufficient specificity to screen for such interactions. Figure 1 summarizes the overall approach used in these experiments.

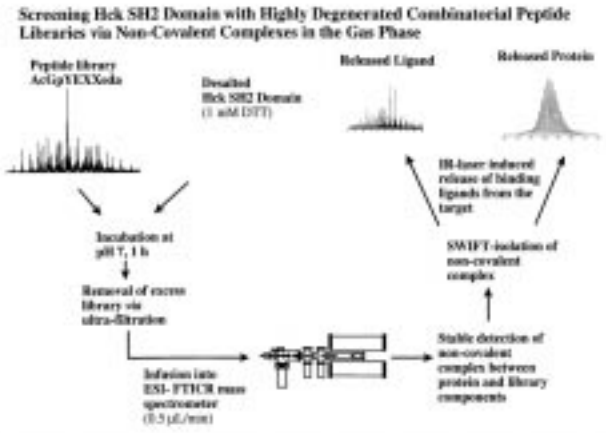

Figure 1. Schematic representation of the use of FTICR mass spectrometry to determine strongest binding components of a combinatorial peptidic library with Hck SH2 domain protein.

Inductively-Coupled Plasma Mass Spectrometry with Ultra-High Mass Resolving Power

Eyler, J.R., UF, Chemistry/NHMFL
Houk, R.S., Iowa State Univ., Chemistry
Bossio, R., FSU, Chemistry
Hendrickson, C., NHMFL
Drader, J., NHMFL
Marshall, A.G., NHMFL/FSU, Chemistry

An inductively coupled plasma (ICP) ion source has been incorporated into Fourier transform ion cyclotron resonance (FTICR) mass spectrometers at both the UF Department of Chemistry and the National High Field FTICR Facility at the NHMFL. This has permitted analyses of elemental species in the presence of both isobaric and polyatomic "interferents" of similar mass to the analyte ions of interest. Initial studies[1] showed quite respectable sensitivities (μg/L detection limits) at high mass resolution (mass resolving powers, $m/\Delta m_{10\%V}$ up to 80,000). During the past year an improved ICP source, which can be used on FTICR instruments at both UF and the NHMFL, was constructed and has provided dramatically improved figures of merit in ICP-FTICR experiments at UF. For example, mass resolving power, $m/\Delta m_{10\%V}$, of 260,000 has been achieved, sufficient for resolving Ca^+ from ubiquitous Ar^+ background ions. Detection sensitivities in the low μg/L range have been found for samples of indium. The 6 T FTICR mass spectrometer in the National High Field FTICR Facility at the NHMFL has been modified to accommodate the new ICP source, and initial experiments led to quite respectable sensitivities and mass resolving powers on it as well.

Reference:

1 Milgram, K.E., *et al*., Anal. Chem., 69, 3714 (1997).

Infrared Multiple Photon Dissociation of Small Peptides

NHMFL

Eyler, J.R., NHMFL/UF, Chemistry
Lang, G.-H.L., UF, Chemistry
Watson, C.H., UF, Chemistry
Marshall, A.G., NHMFL/FSU, Chemistry
Shi, S.D.-H., FSU, Chemistry

Infrared multiple photon dissociation (IRMPD) of small (six or fewer amino acids) arginine-containing peptides was studied using the 9.4 T electrospray ionization (ESI)-Fourier transform ion cyclotron resonance (FTICR) instrument at the NHMFL's National High Field FTICR Facility. General correlations between the dissociation patterns of small peptides and the locations of arginine residues in the peptides were investigated, and the dissociation spectra observed for singly and doubly charged states of the same peptide were analyzed and compared. Dissociation of the same peptides was also studied using sustained off-resonance irradiation (SORI) collisionally activated dissociation (CAD) on a 4.7 T ESI-FTICR instrument at the University of Florida. Figure 1 shows the fragmentation obtained when the singly-protonated tripeptide arginine-glycine-aspartic acid was subjected to infrared radiation from a CO_2 laser.

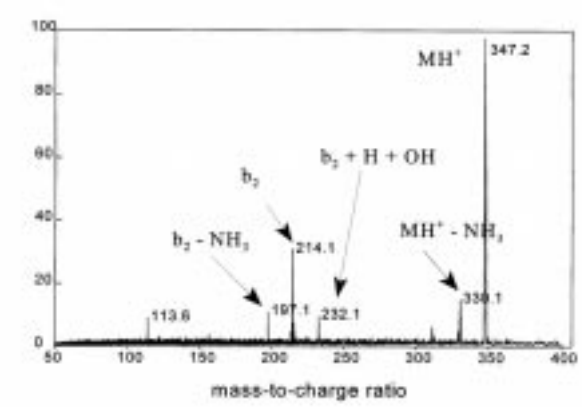

Figure 1. Mass spectrum of protonated arginine-glycine-aspartic acid following IRMPD on 9.4 T magnet at NHMFL.

Study of Motional Dynamics in Complex Fluids by Very High Field, Very High Frequency EPR (VHF-EPR)

Hassan, A.K., NHMFL
Van Tol, J., NHMFL
Maniero, A.L., NHMFL
Brunel, L.-C., NHMFL
Earle, K.A., Cornell Univ., Baker Laboratory of Chemistry
Freed, J.H., Cornell Univ., Baker Laboratory of Chemistry

Very high field/high frequency electron paramagnetic resonance (VHF-EPR) has the potential of allowing us to address important questions about fundamental processes in glass-forming systems as the glass transition is approached. We present experimental VHF-EPR spectra taken with a resistive magnet based high field (25 T) EPR spectrometer at different frequencies (525.4275 and 670.463 GHz) over a temperature range from 200 K to 410 K. Two nitroxide spin probes, perdeuterated 2,2, 6,6-tetramethyl-4-methyl aminopiperidinyl-*N*-oxide (MOTA), and 3,3-dimethyloxazolidinyl-*N*-oxy-2,3-5a-cholestane (CSL) were used in this VHF-EPR study of the glass former ortho-terphenyl (OTP). The observed and simulated EPR spectra of 3 mM CSL in OTP at 525.4275 GHz and 228 K are shown in Figure 1. The following rigid limit parameters were determined for the g and A (hyperfine) tensors from a fit that uses an isotropic Brownian diffusion model with a diffusion rate of 10^6 sec^{-1}: $g_x = 2.009027 \pm 0.000002$, $g_y = 2.006020 \pm 0.000002$, $g_z = 2.002251 \pm 0.000002$, $A_x = 0.591 \pm 0.002$ mT, $A_y = 0.369 \pm 0.002$ mT, and $A_z = 3.380 \pm 0.002$ mT. Figure 2 shows the average rotational diffusion rate, denoted as R^0 for 3mM CSL in OTP at 670.463 GHz, the average rotational rate for 1mM MOTA in OTP at 525.4275 GHz, and the average rotational rates determined for the same MOTA and CSL systems at 250 GHz by Earle, *et al.*[1] The higher frequency data show results for the higher temperatures: They indicate that activated behavior for R^0 observed at 250 GHz continues into the higher

temperature region, although some reduction of this activation energy may take place for CSL. Experiments at lower temperatures and higher frequencies are expected to provide more information, with which to test the microscopic models of dynamics.[1]

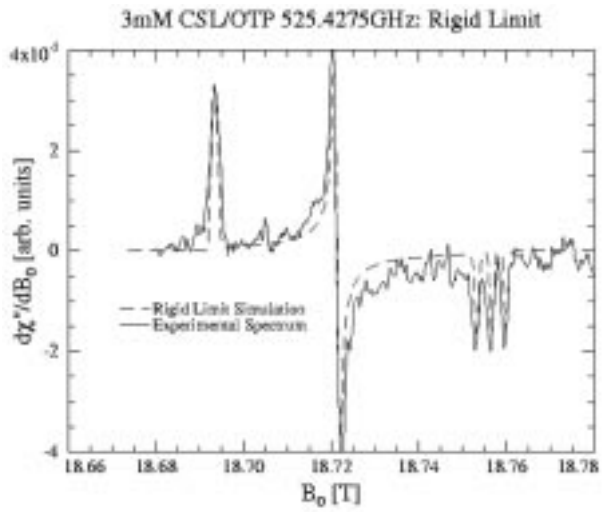

Figure 1. Rigid limit EPR spectra of 3 mM CSL in OTP at 525.4275 GHz and 228 K.

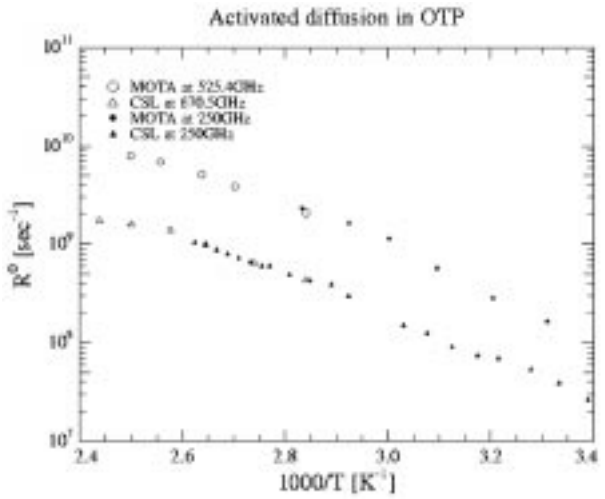

Figure 2. Average rotational diffusion rates as a function of temperature.

Reference:

1 Earle, K.A., *et al.*, J. Chem. Phys., 106, 9996 (1997).

High Frequency and Field EPR of Ferrous Iron in Reduced Rubredoxin Model Compound $Fe(SPh)_4(Ph_4P)_2$

Knapp, M.J., Univ. of California at San Diego, Chemistry
Krzystek, J., NHMFL
Brunel, L.C., NHMFL
Hendrickson, D.N., Univ. of California at San Diego, Chemistry

Iron-sulfur proteins play vital and diverse roles in most living organisms. They are responsible, e.g. for electron transfer, chemical catalysis, iron storage, generation and stabilization of radical intermediates, and site-specific sulfide chemistry. Among the four known categories of iron-sulfur proteins, the simplest one from the structural point of view is the family of electron transfer proteins called rubredoxins. These proteins contain a single iron ion, which is tetrahedrally coordinated by the thiolate groups of each of four cysteinyl ligands from the protein. The iron ion can be either in the reduced (ferrous) or oxidized (ferric) state.

Although the oxidized (Fe^{3+}) rubredoxin proteins have been a subject of successful EPR studies, this has not been the case with the reduced (Fe^{2+}) form of the protein. The main reason is the properties of the ferrous iron, which has been termed "EPR-silent" due to the either diamagnetic ground state (low spin: S=0), or large zero-field splitting(zfs) parameters of the high-spin (S=2) ground state. In the following we are reporting on the first successful EPR study on a model compound, $Fe(SPh)_4(Ph_4P)_2$, which mimics the active site of the reduced rubredoxin molecule.

The high frequency and field EPR (HFEPR) experiments were performed in a 94 GHz to 433 GHz frequency range, and 0 T to 14 T field range, on a sample pressed into a KBr pellet, at 20 K. A typical spectrum at 189 GHz is shown

in Figure 1. The spectrum could be interpreted using the standard spin Hamiltonian:

$$H = g\beta SH + D(S_z^2\text{-}1/3S(S+1)) + E(S_x^2\text{-}S_y^2)$$

The 189 GHz HFEPR spectrum *simulated* using the following spin-Hamiltonian parameters: D =+5.84, E =+1.42 cm^{-1}, $g_x = g_y = 2.08$, $g_z = 2.00$ are shown in Figure 1. The zfs parameters are much closer to the earlier reported far-infrared results (1) than those measured by Mössbauer spectroscopy, (2) which reaffirms the superiority of HFEPR as an experimental technique to investigate high-spin transition metal ions. This is the first time, to the best of our knowledge, that *allowed* spin transitions have been observed in any ferrous iron-containing system, and the first time too that such transitions in a S=2 system with highly rhombic zfs tensor (E/D ~ 0.25) have been observed and successfully interpreted. These results will lead to a better understanding of the electronic structure of reduced rubredoxin molecule.

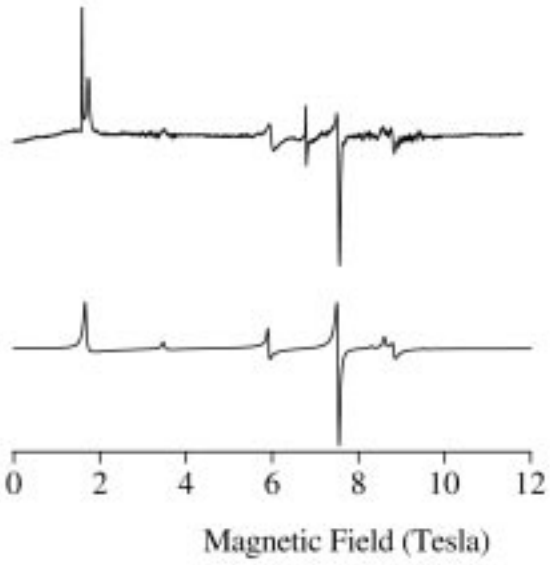

Figure 1. HFEPR spectrum of a $Fe(SPh)_4(Ph_4P)_2$ pellet at 189.38 GHz (top), and the same spectrum simulated using spin-Hamiltonian parameters in the text (bottom). The two sharp peaks at g = 6, and g = 2 in the experimental spectrum are due to a ferric impurity, and not reproduced in the simulation.

References:

1 Champion, P.M., *et al*., Chem. Phys., 66, 1819 (1977).

2 Blake, P.R., *et al*., Biochem., 30, 10885 (1991).

High Frequency and Field EPR Spectroscopy of Resonance Delocalized $[Fe_2(OH)_3(tmtacn)_2]^{2+}$

Knapp, M.J., Univ. of California at San Diego, Chemistry
Krzystek, J., NHMFL
Brunel, L.-C., NHMFL
Hendrickson, D.N., Univ. of California at San Diego, Chemistry

The study of mixed-valence, dinuclear iron complexes have advanced understanding of the role played by these complexes in proteins such as ferredoxin and hemerythrin. The importance of resonance delocalization to the spin-state ordering has become increasingly clear in recent years. Typically, antiferromagnetic exchange is dominant, leading to an $S_T = 1/2$ ground state that is fully characterizable by X-band EPR. In some cases, however, resonance delocalization leads to a net ferromagnetic interaction, and an S = 9/2 ground state. The resonance delocalized model ion $[Fe_2(OH)_3(tmtacn)_2]^{2+}$ was studied by high frequency (110 GHz to 440 GHz), and field (0 T to 14.5 T) EPR (HFEPR) to fully characterize its electronic structure. A full-matrix diagonalization approach was used to derive the spin-Hamiltonian parameters for this S_T= 9/2 complex. Fine structure peaks due to transitions between the Kramers doublets (-9/2 -> -7/2, -7/2 -> -5/2, etc.) were observed in powdered samples. The spacing of the fine structure reveals that the axial zero-field splitting (ZFS) parameter D is positive, and on the order of 1 cm^{-1}. Simulations reveal that the electronic structure can be accounted for by the conventional spin-Hamiltonian:

$$H = g\beta SH + D(S_z^2\text{-}1/3S(S+1)) + E(S_x^2\text{-}S_y^2)$$

with the following set of parameters: D = +1.08 cm^{-1}, |E| < 0.01 cm^{-1}, $g_x = g_y = g_z = 2.00$. The HFEPR spectra reveal multiple allowed inter-Kramers transitions in this S = 9/2 system, permitting a greater understanding of its electronic structure, such as the direct measurement of the ZFS, than was available by conventional EPR spectroscopy where usually only the intra-Kramers transition (-1/2 -> +1/2) has been observed. The successful analysis of HFEPR spectra obtained from powdered samples of this high-spin system is a step toward analyzing high-spin metalloproteins.

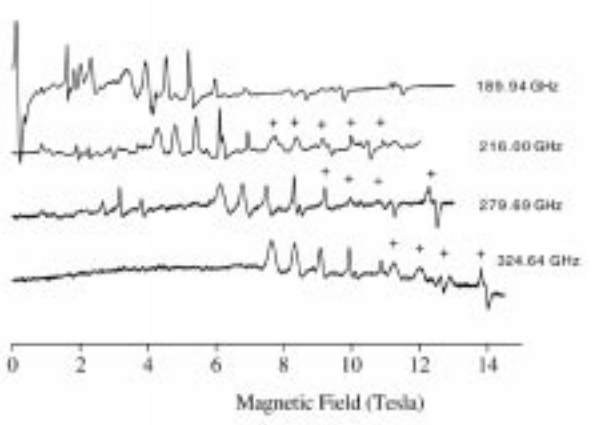

Figure 1. HFEPR spectra of a $[Fe_2(\mu\text{-}OH)_3(tmtacn)_2]^{2+}$ sample pressed in a KBr pellet collected at 20 K over the 189 GHz to 324 GHz frequency range. Each spectrum is labeled with its nominal frequency. Features marked with a "+" arise from a higher harmonic of the fundamental frequency.

EPR from "EPR-Silent" Species: High Frequency and Field EPR Spectroscopy of Manganese(III) in Porphyrinic Complexes

Krzystek, J., NHMFL
Telser, J., Roosevelt Univ., Chemistry
Goldberg, D.P., Johns Hopkins Univ., Chemistry
Pardi, L.A., Univ. of Florence-Italy, Chemistry
Brunel, L.-C., NHMFL
Hoffman, B.M., Northwestern Univ., Chemistry

In our continuing effort to characterize transition metal ions, deemed hitherto "EPR-silent," we performed high frequency and field EPR (HFEPR) studies of Mn^{3+} in its high-spin (S = 2) state ligated by two related complexes: tetraphenylporphyrine (TPP) and phthalocyanine (Pc). In both cases the axial ligand was Cl^-.

The importance of Mn^{3+} lies in the diverse and important roles this ion plays in many biochemical and catalythical reactions. To give an example of a possible application, $Mn(III)P_C$ has been proposed as a building block in molecular magnets.[1] Despite its importance, however, Mn^{3+} has, until recently, been inaccessible to conventional EPR spectroscopy due to its large zero field splitting (zfs) parameters. Only in the last two years several HFEPR reports have appeared.[2,3]

In our previous and preliminary study,[2] we reported a HFEPR study of field-oriented solid sample of Mn(III)TPP. This was so because the large magnetic moment of a single microcrystallite at low temperature causes a torquing effect aligning the specimen along the magnetic field. A resulting single crystal-like spectrum is easy to interpret, however, it does not yield a complete set of spin Hamiltonian parameters. In an effort to produce a HFEPR spectrum of a randomly oriented sample, a way to immobilize the microcrystallites in the magnetic field had to be found. Figure 1 presents a ~280 GHz spectrum of a Mn(III)TPP powder sample that was embedded in eicosane. All the features of this rich spectrum could be identified as either allowed ($\Delta M_s = \pm 1$), or partially allowed ($\Delta M_s = \geq 2$) transitions within the S = 2 manifold. The spin Hamiltonian parameters were obtained by means of simulation using a full-matrix diagonalization, as well as analytical techniques, and are the following: D = -2.27(1), E = 0.0(1) cm^{-1}, $g_{iso} = 2.00$. A simulated spectrum using these parameters is shown in Figure 1, and shows a nearly perfect agreement with the experiment. The corresponding parameters for Mn(III)Pc are: D = -2.34(1), E = 0.0(1) cm^{-1}, $g_{iso} = 2.00$. Currently studies are

being continued to fully characterize the electronic structure of Mn^{3+} in both kinds of complexes. Of particular importance is the need, shown in this study, of a multi-frequency EPR approach to high-spin non-Kramers systems such as Mn^{3+}, since a "window" of frequencies is necessary to observe the optimal number of allowed transitions in such systems. This may not necessarily be the highest frequency accessible.

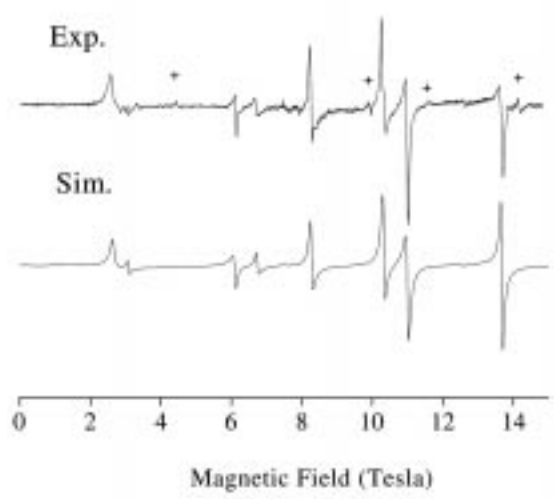

Figure 1. A 279 GHz EPR spectrum of Mn(III)TPP embedded in eicosane at 10 K (top). The transitions marked with a "+" are induced by a higher harmonic of the fundamental source frequency, and are thus not reproduced in the simulated spectrum (bottom).

References:

1 Miller, J.S., *et al*., J. Adv. Mater., 4, 498 (1994).

2 Goldberg, D.P., *et al*., J. Am. Chem. Soc., 119, 8722-8723 (1997).

3 Barra, A.L., *et al*., Angew. Chem. Intl. Ed. Engl., 36, 2329 (1997).

Identification, Composition, and Asymmetric Formation Mechanism of Glycidyl Methacrylate/Butyl Methacrylate Copolymers up to 7,000 Da from Electrospray Ionization Ultrahigh Resolution Fourier Transform Ion Cyclotron Resonance Mass Spectrometry

Marshall, A.G., NHMFL/FSU, Chemistry
Shi, S.D.-H., FSU, Chemistry
Hendrickson, C.L., NHMFL
Simonsick, W.A., Jr., DuPont Marshall Laboratory
Aeserud, D.J., DuPont Marshall Laboratory

Glycidyl methacrylate (GMA) and butyl methacrylate (BMA) have the same nominal mass (142 Da), but differ in exact mass by 0.036 Da (CH_4 *vs.* O). Therefore, copolymers formed from the two isobaric monomers exhibit a characteristic isobaric distribution due to different monomer compositions. We have shown that electrospray ionization FT-ICR mass spectrometry at 9.4 T resolves the isobaric components of copolymers as large as 7,000 Da with a resolving power ($m/\Delta m_{50\%}$) of ~500,000 in a gel permeation chromatography fractionated polymer sample. That resolution provides for complete and unequivocal component analysis of such copolymers of the size used for high solid content automobile coatings. All five possible copolymer products predicted by the polymerization mechanism are resolved and identified in the mass spectrum. Two of those polymer series (each with saturated end group) were previously unresolved by mass spectrometry because they differ in mass from the two other unsaturated products by only 0.0089 Da. Finally, analysis of the asymmetrical isobaric distribution for the copolymer n-mers, $(GMA)_m(BMA)_{n-m}$, $0 \le m \le n$, in which species with adjacent values of m differ from each other in mass by 36 mDa (i.e., the mass difference, CH_4 vs. O, between GMA and BMA)

proves that GMA is less reactive than BMA in the polymerization process (see Figure 1).[1] Thus, for the first time, it becomes possible to resolve, identify, and quantitate all (five in this case) of the possible copolymer variants, as well as to determine which of the two monomer units has the greater tendency to polymerize.

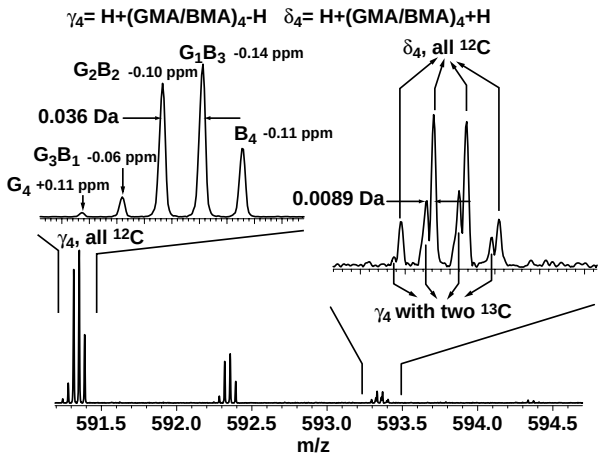

Figure 1. Ultrahigh resolution FT-ICR mass spectrum and accurate mass measurements for the GMA/BMA tetramer. Note the asymmetric isobaric distribution (left) and the resolution of the saturated (δ_4) species from the unsaturated (γ_4, containing a carbon-carbon double bond) species with two ^{13}C (right).

Reference:

1 Shi, S.D.-H., *et al*., Anal. Chem., 70, 3220-3226 (1998).

Resolution, Elemental Composition, and Simultaneous Monitoring by Fourier Transform Ion Cyclotron Resonance Mass Spectrometry of Organosulfur Species Before and After Diesel Fuel Processing

Marshall, A.G., NHMFL/FSU, Chemistry
Rogers, R.P., FSU, Chemistry
White, F.M., FSU, Chemistry
McIntosh, D.G., NHMFL
Andersen, K.V., Haldor Topsoe (Denmark)
Hendrickson, C.L., NHMFL

Elemental compositional analysis of processed and unprocessed diesel fuels has been obtained with a 5.6 T Fourier transform ion cyclotron resonance (FT-ICR) mass spectrometer coupled to an all-glass heated inlet system (AGHIS).[1] High resolution mass spectra of electron-ionized diesel fuel samples could be obtained from as little as a 500 nL septum injection into the AGHIS, to yield ~500 peaks over a range, $90 < m/z < 300$, with as many as 7 peaks present at the same nominal mass. Molecular formulas (elemental compositions) are assigned from accurate mass measurements with an average error less than ±0.5 ppm.

Comparison of the raw and processed diesel spectra (e.g., Figure 1) showed complete removal of the sulfur-containing species except for dimethyldibenzothiophene and higher alkyl-substituted dibenzothiophenes. These results confirm prior reports of the resistance of these species to hydrotreatment due to steric hindrance of catalytic desulfurization arising from 4,6 dimethyl substitution (see Figure 1). A simple liquid chromatographic separation to isolate N-, O-, and S-containing aromatics from processed diesel fuel simplifies the mass spectrum, and extends the dynamic range of the analysis, making it possible to identify many nitrogen and oxygen

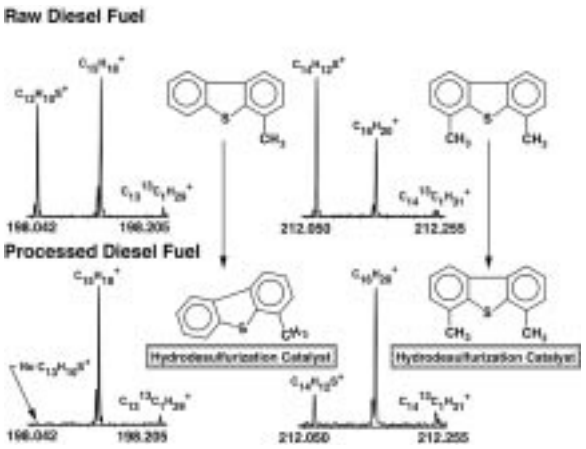

Figure 1. Electron ionization FT-ICR mass spectra of methyldibenzothiophene (left) and dimethyldibenzothiophene (right) before (top) and after (bottom) hydro-desulfurization. Note the complete catalytic removal of methyldibenzo-thiophene, but incomplete removal (due to steric hindrance for the 4,6-isomer) of dibenzothiophene.

homologs of the sulfur-containing species, as well as confirm the presence of sulfur-containing species initially detected in the unfractionated processed diesel fuel.[2]

These results provided the first direct evidence for a proposed steric hindrance mechanism in catalytic hydrodesulfurization of diesel fuel. The technique development aspects of this work have been featured by *Analytical Chemistry*.[3]

References:

1 Rodgers, R.P., *et al*., Rev. Sci. Instrum., 69, 2278-2284 (1998).
2 Rodgers, R.P., *et al*., Anal. Chem., 70, 4743-4750 (1998).
3 Anal. Chem., 70, 567A-568A (1998).

The Discrete Frenet Frame and Coiled Coil Proteins

Quine, J.R., NHMFL/FSU, Mathematics
Denny, J.K., NHMFL/FSU, Mathematics

The coiled coil is a supersecondary protein structure that occurs in helix bundles, such as collagen and leucine zippers. Coiling also appears to be a feature of proteins forming ion channels. The models developed by Pinto, *et al*.,[1] and by Samson, *et al.*,[2] of the transmembrane segment of the M2 peptide in the influenza A virus, which have a coiled coil structure and form bundles, are based on heptad repeat units similar to those seen in leucine zippers.

Models of protein backbone structures can be viewed as polygonal paths in space with vertices representing atom locations and with exterior angles that satisfy bond angle constraints dictated by the chemical bonding at each atom. In contrast to continuous mathematical models of coiled coils, our work presents a mathematical model based on the discrete Frenet frame (DFF) and Chasles's formula for the axis of an Euclidean motion. The discrete Frenet frame provides a method for investigating curvature and torsion of a polygonal path in space by defining tangent, normal, and binormal vectors at each vertex. For protein backbones, the discrete analogue of the curvature relates to the known bond angles and lengths, and the discrete analogue of torsion relates to the usual Φ, Ψ and ω torsion angles.

The DFF is used to explore coiling, and to analyze the structure of ideal α-helices, β-helices, coiled coils, and other periodic structures that satisfy bond angle and bond length constraints. With the DFF, coiling can be realized as a periodicity in generating the discrete Frenet frame. The most common periodicity is a repeat unit of three atoms, since the peptide bond tends to be planar. Other periodicities seen in proteins include: the 2 peptide plane repeat unit in LD-helices (such as gramicidin A), the 9 atom repeat unit in collagen, and the 7 peptide plane repeat unit seen in leucine zippers. Moreover, Harbury, *et al*.[3], recently engineered a protein to have an 11 peptide plane period. To compute various parameters for such coils, we have discovered that Chasles's formula for determining the axis of a screw rotation is useful. Formulas are given for the radius and angle of coiling in terms of the free parameters and used to create periodic protein backbones with any degree of coiling. These methods are applied to create models of 4-helix

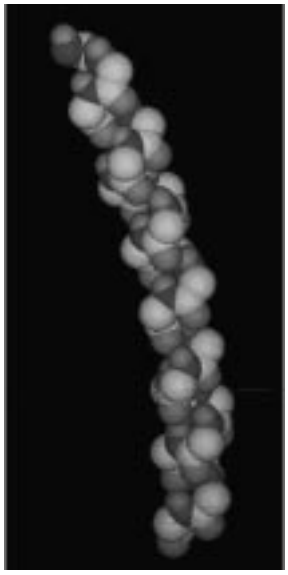

Figure 1. A simulated coiled coil with a seven peptide plane repeat unit generated using the discrete Frenet frame and Euclidean motions.

bundles similar to those seen in the transmembrane segment of the M2 protein of influenza A and to compare calculated NMR data from them to the observed data. These methods are also applicable to LD helices.[4]

References:

1 Pinto, L.H., *et al.*, Proc. Natl. Acad. Sci. U.S.A., 94, 11301-11306 (1997).
2 Samson, M.S.P., *et al*., Virology, 233, 163-173 (1997).
3 Harbury, P.B., *et al*., Science, 282, 1462-1467 (1998).
4 Quine, J.R., Theochem. (1998).

HF-EPR of Irradiated 10-Nondecanone in Perhydrotriphenylene Inclusion Compound

Segre, U., Univ. of Modena-Italy, Chemistry
Maniero, A.L., NHMFL
Brustolon, M., Univ. of Padova-Italy, Physical Chemistry
Brunel, L.C., NHMFL

The recognition of the importance of high frequency EPR in elucidating structural properties of paramagnetic molecules is now quite widespread. The larger value of the Zeeman interaction causes also a change in the characteristic spectroscopic timescale. As a consequence, the dynamics of the radicals in an HF EPR experiment appears slowed down with respect to X band spectra. This effect is of great importance when the motion—on the timescale of the low frequency spectroscopy—is so fast that modulation of the g tensor anisotropy is not effective in relaxing the spin magnetization.

We have studied for some time the properties of radicals obtained by γ irradiating inclusion compounds formed by long chain hydrocarbon derivatives as guest inside host matrices that, like urea and perhydrotriphenylene (PHTP), have hexagonal, non-intersecting channels.[1-5] The radicals are always formed by breaking of a C-H bond next to the functional group. Recently we have compared the properties of the radical obtained by γ irradiation of nonadecan-10-one (10-NDO) included in urea and PHTP in the temperature range 160 K to 300 K.[5] The radical rotates rapidly along the channel axis in both compounds and the analysis of the EPR line width gives information on its correlation time. It has been found that the radical in PHTP rotates faster than in urea and the correlation time for T>200 K is so short that this relaxation mechanism contributes negligibly to the X band EPR line width.

In this report we extend the analysis of the rotational motion of 10-NDO in PHTP thanks to HF EPR spectroscopy in the W band region. X and W band EPR spectra are shown in Figures 1 and 2. The comparison of the spectra recorded at the same temperature shows that the lineshape is broadened at higher frequency. Both series of spectra can be interpreted with a first order, fast-motion analysis. The motional correlation times are inside the fast motion region for X band spectra from room temperature down to T=160 K, where a structural phase transition occurs. On the contrary, as a consequence of the slowing down effect of the HF EPR, the W band spectra have a first order line shape in a narrower temperature range and a T=200 K the spectrum has nearly the same line shape as the X band spectrum at T=160 K.

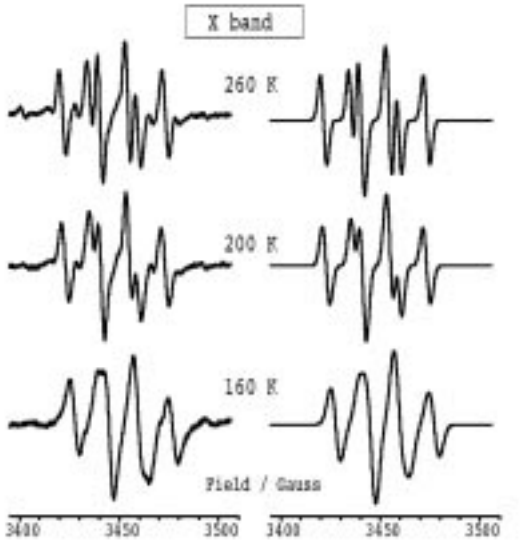

Figure 1. X band spectra recorded with the magnetic field orthogonal to the channel axis together with their best-fit simulation (right).

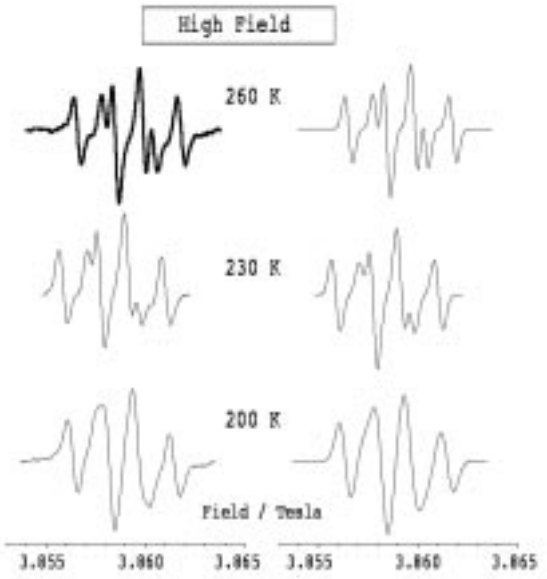

Figure 2. W band spectra as in Figure 1.

The values of the line splittings and of the line widths are obtained with a least square fitting procedure. Each line of the EPR spectrum is labeled by the spin quantum numbers M_k of the coupled nuclei and its width is given by a polynomial expansion: $\delta = A + \Sigma_k B_k M_k + \Sigma_k C_k M_k^2 + \Sigma_{kk'} E_k M_k M_{k'}$.

The values of the line width coefficients are related to the different relaxation mechanisms. The modulation of the Zeeman interaction contributes to the A coefficient, while the cross correlation between the Zeeman and the hyperfine interaction tensors contributes the B_k terms. Therefore, the A and B_k coefficients depend on the intensity of the magnetic field H_0.

We focused our attention on the B_α coefficient, for which the following theoretical expression is obtained: $B_\alpha = (\pi \mu_B \Delta g \Delta A_\alpha / 2h)\tau_c H_0$, where μ_B is the Bohr magneton, Δg and ΔA_α are the anisotropies of the relevant tensors in the molecular plane orthogonal to the channel axis, and τ_c is the correlation time for the molecular rotation about the channel axis.

The values of the B_α coefficients measured at X and W band are reported in Figure 3 as a function of the temperature. The B_α coefficient is not vanishing outside of the error range only in a limited temperature interval whose extension depends on the strength of the magnetic field. The X band data can be exploited in the low temperature limit (T<170 K), while the W band values are significant in the intermediate region, and still higher frequencies should be used to obtain sets of values for the high temperature limit (T>250 K). For that the two sets of measurements can be merged to obtain the values of the correlation time τ_c in a wide range of temperatures. It is readily visible from the data displayed in Figure 3 that the rotational motion of 10-NDO in PHTP is an activated process with activation energy E_r / k = 1300 K. The correlation time is 3×10^{-12} s at room temperature (290 K). It is also evident that this results could be affected by a large error if a single set of measurements is used, for instance only the low or only the high field data.

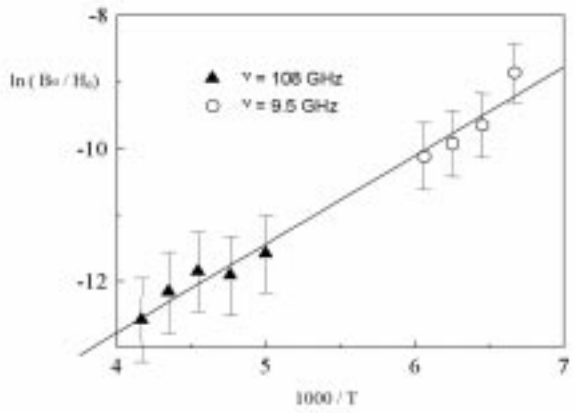

Figure 3. Logarithmic plot of the ratio B_α / H_0 against the reciprocal temperature: (▲) W band data; (O) X band data.

In conclusion, the analysis of the relaxation effects shows that both low frequency (X band) and higher frequency (W band) data are necessary to obtain the maximum of information on the molecular dynamics.

References:

1 Bonon, F., *et al.*, Appl. Magn. Reson., 3, 779 (1992).
2 Segre, U., *et al.*, J. Phys. Chem., 97, 2904 (1993).
3 Brustolon, M., *et al.*, J. Mater. Chem., 6, 1723 (1996).
4 Brustolon, M., *et al.*, Perkins Trans., 2, 2519 (1997).
5 Brustolon, M., *et al.*, Perkins Trans., 2, 1731 (1998).

Influence of Magnetic Field in Electrodeposition Reactions

Spada, F., Univ. of California at San Diego, Center for Magnetic Recording Research
Coey, M., Trinity College, Dublin, Ireland, Physics

Previous studies[1,2,3] and references therein have demonstrated that the electrodeposition rate of copper is enhanced in the presence of a magnetic field. The origin of field effects on electrodeposition has been attributed to lowered deposition overvoltage, altered ion concentration immediately adjacent to the electrode surface,[2] and increased convection currents arising from the Lorentz force acting on charged species in solution.[4] More recent work[3] has demonstrated a dramatic increase of the field-assisted deposition rate when solution pH is below ~1. Our research at the NHMFL extended this latter work by focusing on how the copper electrodeposition rate varied with magnetic field strength in low pH 0.75M copper sulfate solutions. We performed copper plating experiments in 0 T to 6 T fields using the wide bore 6 T superconducting magnet. As shown in Figure 1 the cathodic current density (which is proportional to the rate of copper reduction) at -0.5 V increases fivefold with field between 0 T and 6 T, with the enhancement effect appearing to saturate in the 5 T to 6 T range. The effect of field is greatly diminished at pH 3.5 (Figure 2), as previously reported.[3] No influence of the field direction was observed in our studies. Although these significant field-induced effects are thought to have magnetohydrodynamic origins, more work will be required to establish the underlying mechanisms.

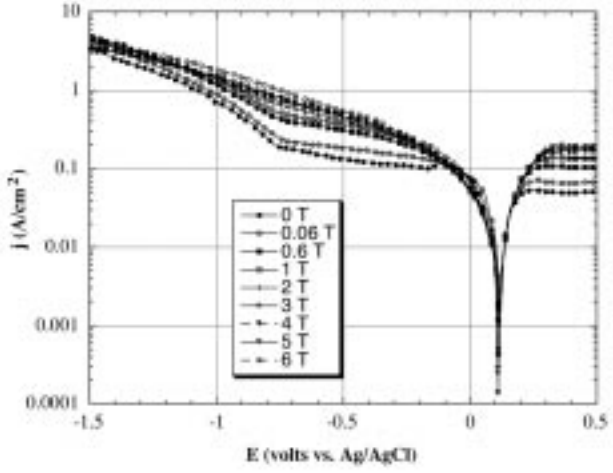

Figure 1. Plots of current density vs. applied potential at various field strengths for a copper electrode in 0.75M copper sulfate solution at pH 0.5.

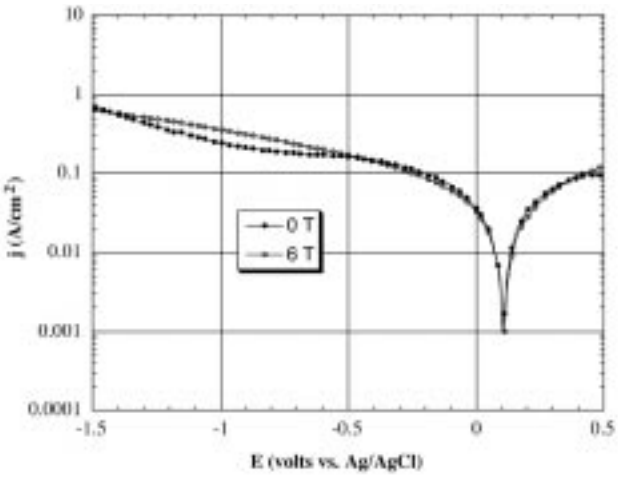

Figure 2. Plots of current density vs. applied potential at 0 T and 6 T for a copper electrode in 0.75M copper sulfate solution at pH 3.5.

References:

1 Chopart, J.P., *et al*., Electrochimica Acta, 36, 459 (1991).
2 Noninski, V.C., Electrochimica Acta, 42, 251 (1997).
3 Hinds, G., *et al*., J. Appl. Phys., 83, 6447 (1998).
4 Ragsdale, S.R., *et al*., J. Phys. Chem., 100, 5913 (1996).

Kinetics of Formation of Xenon Hydrate Clathrate: Hyperpolarized Xenon-129 NMR Studies

Storhaug, V., UF, Chemistry
Liebig, F., UF, Chemistry
Bowers, C.R., NHMFL/UF, Chemistry

The hydrate clathrates are a class of solids guest molecules occupy cages in a host structure formed from H-bonded water molecules. The normally unstable empty clathrate is stabilized by inclusion of the guest. While the general crystal structure of

the type-I hydrate clathrates has already been established, the proposed mechanism for their nucleation and growth awaits experimental confirmation. This being our objective, we have studied both the melting and kinetics of formation of type-I xenon hydrate clathrate using hyperpolarized xenon-129 NMR. The >2000 fold signal enhancement afforded by this method permits single scan observation of cage formation at less than parts-per-thousand levels. The signals arising from xenon-129 enclathrated in the large and small cages are well resolved, permitting the time dependence of each type to be measured independently. Our kinetic model incorporates the time variations of the densities of the gaseous Xe, the Xe enclathrated into the small and large cages, and the xenon-129 magnetization of all three species. The observed induction period in the pressure and NMR data from 203 K to 263 K support a mechanism whereby the hydrate nucleates at sites presumed to be small cages. The nucleation sites then serve as templates for the formation of large and additional small cages. This mechanism is consistent with recent molecular dynamics simulations of the formation process and melting process.

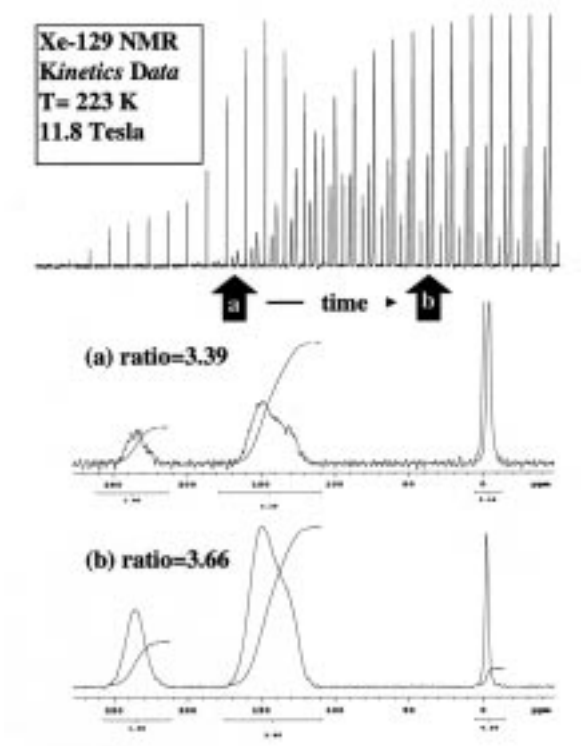

Figure 1. Top: Horizontal array of hyperpolarized xenon-129 NMR spectra obtained as a function of time following the mixing of hyperpolarized xenon gas with ice crystals at a temperature of -50 C. (a,b) left peak: xenon enclathrated into small hydrate cages middle peak: xenon in large hydrate cages, right peak: xenon gas peak. During the course of the reaction the ratio of large to small xenon cages changes increases to a value of 3.66, which is well above the stoichiometric ratio of 3:1.

EPR from "EPR-Silent" Species: High Frequency and Field EPR Spectroscopy of Aqueous Chromium(II)

Telser, J., Roosevelt Univ., Chemistry
Pardi, L.A., Univ. of Florence-Italy, Chemistry
Krzystek, J., NHMFL
Brunel, L.-C., NHMFL

EPR spectroscopic methods at conventional microwave frequencies have been fruitfully employed in determining the structural and electronic environments of half-integer-spin (Kramers) paramagnets. These methods, however, are not applicable to systems with integer-spin (non-Kramers) ground states, where the zero-field splitting (zfs) is larger than the microwave quantum, in particular, where the zfs interaction approaches axial symmetry. The recently developed technique of high frequency, high field EPR (HFEPR; ν> 90 GHz) has now proven to be effective at elucidating the electronic structure of integer-spin systems.[1-3] Of particular value is the combination of the multi-frequency capability of the EPR spectrometer employed here with the ability to perform continuous field sweeps over a broad range (0 T to 17 T). This allows one to choose a convenient parameter "window" to observe most, if not all, of the multitude of transitions characterizing a high-spin, non-Kramers spin species.

We report here the use of HFEPR to investigate a classic "EPR-silent" non-Kramers system, aqueous Cr^{2+} (high-spin: $3d^4$, $S = 2$). We selected this system for its inherent interest as a high-spin system with

Jahn-Teller distortion, and because a significant amount of background information on it exists.

Figure 1 presents a typical HFEPR spectrum of aqueous Cr^{2+} at ~330 GHz. This very rich spectrum has been interpreted by a detailed analysis based on a combination of analytical and full-matrix solutions to the spin Hamiltonian for an $S = 2$ system. The resulting Hamiltonian parameters are: $D = -2.20(5)$ cm^{-1}, $E = 0.0(1)$, and $g_{||} \sim g_{\perp} = 1.98(2)$, independent of solvent system and counterion. These results are in agreement with an early single-crystal EPR study of $CrSO_4{\cdot}5H_2O$[4]. The present study, however, allows unequivocal determination of the sign of D, and shows that in solution, $[Cr(H_2O)_6]^{2+}$ is a perfectly axial system (tetragonally elongated), as opposed to solid $CrSO_4{\cdot}5H_2O$, which showed a measurable E value, indicative of slight orthorhombic distortion as seen in its crystal structure. HFEPR data is combined with earlier electronic absorption data to provide a complete picture of the electronic structure of Cr^{2+} in this chemical environment. The present study also shows the applicability of high field EPR to aqueous solutions of integer-spin ("EPR-silent") transition metal complexes, as previous studies have employed only solid (single-crystal or polycrystalline) samples.

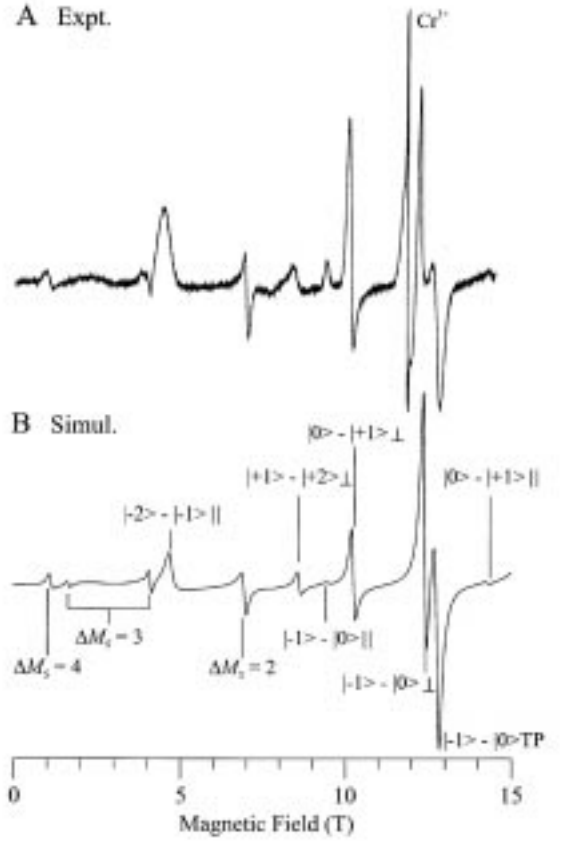

Figure 1. HFEPR spectrum of aqueous Cr^{2+}, sulfate counterion at 328.69 GHz and 10 K: (A) experimental spectrum. (B) spectrum simulated using parameters as in text. Individual allowed and partially allowed transitions are identified. The sharp peak at g = 2 is due to a Cr^{3+} impurity, and is not reproduced in the simulation.

References:

1 Goldberg, D.P., *et al.*, J. Am. Chem. Soc., 119, 8722 (1997).
2 Barra, A.L., *et al.*, Angew. Chem. Intl. Ed. Engl., 36, 2329 (1997).
3 Telser, J., *et al.*, Inorg. Chem., 37, 5769 (1998).
4 Ono, K, *et. al.*, Phys. Rev., 96, 38 (1954).

Water: A "Foldase" That Catalyzes Hydrogen Bond Exchange in Polypeptide Conformational Rearrangements

Xu, F., NHMFL/FSU, Chemistry
Cross, T.A., NHMFL/FSU, Chemistry and Molecular Biophysics

The polymorphic nature of gramicidin, a polypeptide that forms a cation channel in membranes, permits a wide range of studies. In organic solvents this molecule typically forms an intertwined dimeric helix. The helix can be left-handed or right-handed, it can also be parallel or antiparallel. Moreover, under specific circumstances the structure can "slip" in register so that the two monomers are staggered with respect to each other. In fact, in crystallization such staggered structures can form long cylindrical structures. They can also change the number of residues per turn, thus expanding or contracting the pore dimensions on the helical axis. In a lipid environment, one conformation dominates all others, a single-stranded dimer with 6.5 residues per turn, forming a pore of approximately 0.3 nm in diameter.

Here we have taken advantage of this polymorphism to look at how structures can interconvert in a low dielectric environment. The motivation for this work is the challenging task of trying to determine how molecular structures fold in a low dielectric environment, such as a lipid bilayer or the interstices of the hydrophobic core of a water soluble protein. It has been shown that a variety of double helical conformations can be kinetically trapped in a non-protic organic solvent, such as dioxane. In the presence of a minimum amount of water, about three molecules per gramicidin dimer, the conversion rate of a parallel conformation to the antiparallel minimum energy conformation in this environment takes more than 1500 hours. These results were determined by observing the fingerprint region of GCOSY solution NMR spectra. As shown in Figure 1, this rate is highly dependent on the concentration of water present. Indeed the rate of interconversion increases in proportion to $[H_2O]^{6.5}$.

We have previously shown that protic solvents not only bind to the hydrophilic indole N-H groups on the surface of these dimeric structures, but they also bind to the amide backbone. To convert from one structure to another the hydrogen bonds between amide groups must be broken and allowed to reform. We hypothesize that these intertwined helices can "unscrew" from each other requiring 10 pairs of hydrogen bonds to be broken. Water can participate by binding to these amide sites, destabilizing the hydrogen bonds, and then stabilizing the reaction transition state, the unbonded donor and acceptor. Hence, the water acts as a catalyst to lower the activation delta free energy in just the same way that other catalysts enhance reaction rates. Indeed, the comparison is striking with a class of protein catalysts called, protein disulfide isomerases, which enhance protein folding rates by breaking disulfide bonds on misfolding pathways. In fact, these isomerases enhance folding rates by two to four orders of magnitude, the same order of magnitude as seen here for the catalytic effect of water on breaking hydrogen bonds.

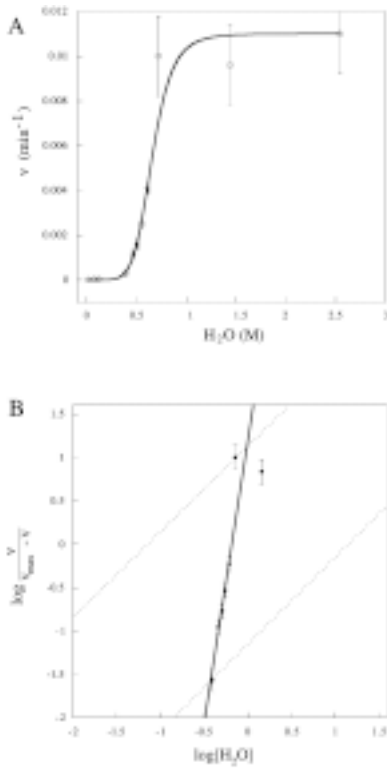

Figure 1. The initial conformational interconversion rates as a function of water concentration. The rate constants were measured from buildup curves of the fully assigned resonances for the antiparallel conformer, and they range from 1.4 x 10^{-5} to 1.0 x 10^{-2} min^{-1}. The much increased error bars for the faster rates reflect the time required for acquiring the initial GCOSY data set for each sample (~18 min.). The Hill plot with a slope of 6.5 indicates a very substantial cooperation for the catalytic activity of water, suggesting that the breaking of one pair of peptide H-bonds readily leads to the subsequent disrupting of neighboring and next nearest neighboring H-bond pairs. The data corresponding to 3% to 95% kinetic rate saturation are used for calculating the maximal slope for the Hill coefficient.